

# Computed Tomography and Magnetic Resonance Imaging Manifestations of Spinal Monostotic Fibrous Dysplasia

Yu Zhang, Chuanyu Zhang, Shaohua Wang, Hexiang Wang, Yupeng Zhu, Dapeng Hao

Department of Radiology,  
The Affiliated Hospital of  
Qingdao University, Qingdao,  
China



Received : 25-03-2018  
Accepted : 20-05-2018  
Published : 18-06-2018

## INTRODUCTION

Fibrous dysplasia (FD) is a benign bone lesion originally described by Lichtenstein and Jaffe in 1942.<sup>[1,2]</sup> According to the literature, FD represents approximately 7% of all benign tumor-like bone lesions.<sup>[3,4]</sup> Depending on the extent of involvement, FD can be divided into two types: monostotic FD (MFD) and polyostotic FD (PFD).<sup>[5]</sup> FD is usually found in the ribs, the proximal femur, tibia, humerus, and craniofacial bones.<sup>[5]</sup> Only 2.5% of FD occurs in the spine.<sup>[3]</sup> Spinal involvement occurs mostly in PFD, and it is unusual for it to occur in MFD.<sup>[3,6]</sup> Treatment of spinal MFD depends on the presence and severity of symptoms. Asymptomatic patients with stable lesions only need clinical observation.<sup>[7-9]</sup> Therefore, a correct preoperative diagnosis of spinal MFD is important to avoid unnecessary surgery.

## ABSTRACT

**Aim:** The purpose of the study was to analyze and summarize the computed tomography (CT) and magnetic resonance imaging (MRI) findings of spinal monostotic fibrous dysplasia (MFD) as well as evaluate the clinical value of CT and MRI in MFD diagnosis. **Materials and Methods:** CT ( $n = 4$ ) and MRI ( $n = 5$ ) images of six patients with pathologically confirmed spinal MFD were examined. The assessed image features included location, shape, rib involvement, vertebral collapse, margin, attenuation, and sclerotic rim on CT, as well as signal intensity, dark signal rim, and enhancement pattern on MRI. **Results:** In total, four of six patients underwent CT scanning. The most common findings on CT scanning were expansile lesions ( $n = 4$ ), sclerotic rims ( $n = 4$ ), and ground-glass opacity (GGO) ( $n = 4$ ). In total, five of six patients underwent MRI. The lesions were low-signal intensity ( $n = 2$ ), low-to-isointense signal intensity ( $n = 1$ ), and low-signal intensity with several isointense portions ( $n = 2$ ) on T1-weighted imaging (T1WI). The lesions were low-signal intensity ( $n = 1$ ), isointense to high intensity ( $n = 1$ ), and isointense signal intensity with several high portions ( $n = 3$ ) on T2WI. A dark signal rim was found in most cases on T1WI and T2WI ( $n = 4$ ). The lesions ( $n = 2$ ) showed obvious enhancement. **Conclusions:** The CT and MRI manifestations of spinal MFD have the following characteristics: expansile lesion, GGO, sclerotic rim, and no obvious soft-tissue mass. The combined use of CT and MRI examinations is necessary for patients with suspected spinal MFD.

**KEYWORDS:** *Computed tomography, magnetic resonance imaging, monostotic fibrous dysplasia, spine*

The purpose of this study was to assess the characteristic computed tomography (CT) and magnetic resonance imaging (MRI) findings of spinal MFD and to evaluate the clinical value of CT and MRI in MFD diagnosis.

## MATERIALS AND METHODS

### Patients

This study was approved by the institutional ethics committee. Since it was a retrospective study,

**Address for correspondence:** Dr. Dapeng Hao,  
Department of Radiology, The Affiliated Hospital of Qingdao  
University, 59 Haier Road, Laoshan District,  
Qingdao, 266071, China.  
E-mail: haodp\_2009@163.com

This is an open access journal, and articles are distributed under the terms of the Creative Commons Attribution-NonCommercial-ShareAlike 4.0 License, which allows others to remix, tweak, and build upon the work non-commercially, as long as appropriate credit is given and the new creations are licensed under the identical terms.

For reprints contact: reprints@medknow.com

**How to cite this article:** Zhang Y, Zhang C, Wang S, Wang H, Zhu Y, Hao D. Computed tomography and magnetic resonance imaging manifestations of spinal monostotic fibrous dysplasia. J Clin Imaging Sci 2018;8:23. Available FREE in open access from: <http://www.clinicalimagingscience.org/text.asp?2018/8/1/23/234658>.

### Access this article online

#### Quick Response Code:



**Website:**  
[www.clinicalimagingscience.org](http://www.clinicalimagingscience.org)

**DOI:** 10.4103/jcis.JCIS\_20\_18

informed consent was not required. In April 2010 to May 2017, a total of six patients with pathologically confirmed spinal MFD were retrospectively reviewed. The patients included three males and three females (age 22–77 years, median age 48.7 years). The clinical symptoms included backache ( $n = 3$ ) and numbness of the limbs ( $n = 1$ ). The remaining lesions were found by routine examination ( $n = 2$ ). The duration of symptoms ranged from 1 month to 20 years (median, 7 months).

### Imaging techniques

CT examinations ( $n = 4$ ) were performed using the standard CT protocol. The imaging parameters were as follows: field of view (FOV) of 200–400 mm, matrix of  $512 \times 512$ , thickness of 1.5 mm, and a reconstruction interval of 1 mm.

MRI examinations ( $n = 5$ ) were performed using a 1.5T MRI scanner (Signa Advantage Horizon; GE Medical Systems, Milwaukee, WI). Both axial and sagittal T1-weighted imaging (T1WI) (500–700 ms repetition time [TR], 15–30 ms echo time [TE], 200–360 mm FOV,  $256\text{--}512 \times 208\text{--}512$  matrix) and turbo spin echo T2WI (3000–5000 ms TR, 60–90 ms TE, 200–360 mm field of view,  $256\text{--}512 \times 208\text{--}512$  matrix) were performed on MRI.

Two cases underwent enhanced MRI. Contrast-enhanced T1-weighted spin-echo images with fat saturation were obtained after the intravenous injection of 0.1 mmol/kg of gadolinium dimeglumine.

### Imaging analyses

All the images were reviewed by two senior radiologists. The reviewers did not know the clinical and histopathological findings of the patients. The criteria for the evaluation of the disease included the lesion location (cervical vertebra, thoracic vertebra, or lumbar vertebra) (vertebral body, vertebral pedicle, or posterior element), shape (circular or irregular), rib involvement (yes or no), and vertebral collapse (yes or no). Margin (well-defined or ill-defined), attenuation (high, low, intermediate, or mixed density), and the sclerotic rim (yes or no) of the lesion were examined on CT. Signal intensity (high-, low-, or intermediate-signal intensity), dark signal rim (yes or no), and the enhancement pattern (mild or obvious) of the lesion were examined on MRI. The signal intensity of the lesion was compared with the spinal cord on MRI. Any differences of opinion were resolved by discussion.

## RESULTS

### General features of the lesions

The CT and MRI imaging features of six patients with spinal MFD were summarized in Table 1. In all six cases,

the lesions occurred in the cervical vertebra ( $n = 2$ ), thoracic vertebra ( $n = 3$ ), and lumbar vertebra ( $n = 1$ ). In addition to one lesion involving vertebral body, vertebral pedicle, and posterior element, at the same time, the rest of lesions were confined in the vertebral body. The shape of the lesions was regular ( $n = 4$ ) or irregular ( $n = 2$ ). One case occurred in the thoracic vertebra with rib involvement. Two cases had vertebral collapse [Figures 1a-c and 2a-d]. The morphology of the lesion was assessed in each case.

### Computed tomography findings

The most common findings on CT scanning were expansile lesions ( $n = 4$ ), sclerotic rims ( $n = 4$ ), and ground-glass opacity (GGO) ( $n = 4$ ). All lesions were well defined ( $n = 4$ ) [Figure 3d-e]. All lesions showed low density, and a sclerotic rim ( $n = 4$ ) [Figure 2a]. The bone cortex was thin ( $n = 4$ ). The adjacent bone was not involved in any cases ( $n = 4$ ). No obvious soft-tissue masses were found in any cases ( $n = 4$ ).

### Magnetic resonance imaging findings

On MRI, the lesions were low-signal intensity ( $n = 2$ ) [Figure 2b], low-to-isointense signal intensity ( $n = 1$ ) [Figure 1a], and low-signal intensity with several isointense portions ( $n = 2$ ) [Figure 3a] on T1WI. The lesions were low-signal intensity ( $n = 1$ ) [Figure 1b], isointense-to-high intensity ( $n = 1$ ) [Figure 2c], and isointense signal intensity with several high portions ( $n = 3$ ) [Figure 3b] on T2WI. A dark signal rim was found in most cases on T1WI and T2WI ( $n = 4$ ) [Figure 3a and b]. The lesions ( $n = 2$ ) showed obvious enhancement on enhanced MRI [Figures 3c and 2d].

### Pathological changes

Histologically, the lesions had the delicate trabeculae of immature bone, with no osteoblasts. The delicate trabeculae floated in immature mesenchymal cells. Cellular fibrous tissue containing a proliferation of spindle cells could be found, and there were no features of malignancy [Figures 3f and 4].

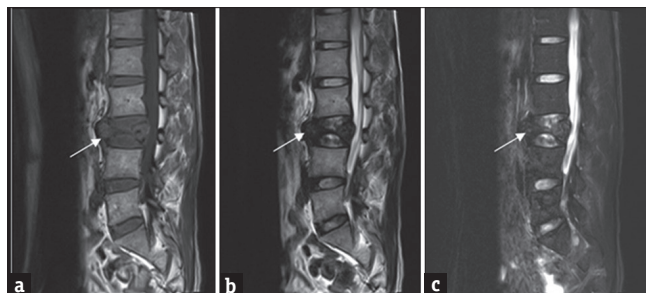


**Figure 1:** A 22-year-old male with monostotic fibrous dysplasia in L3 (original). (a-c) Sagittal T1-weighted imaging, T2-weighted imaging, and T2-weighted imaging-fast spin magnetic resonance imaging showed severe collapse of the vertebral body. Note that the adjacent intervertebral space was not involved.

**Table 1: The results of computed tomography/magnetic resonance imaging findings of spinal monostotic fibrous dysplasia in 6 patients**

Patient/age (years)/sex	CT/MRI image	Site	Shape	Rib damage/ vertebral collapse	CT				MRI			
					Margin	Attenuation	GGO	Sclerotic rim	T1WI <sup>a</sup>	T2WI <sup>a</sup>	Dark signal rim	Enhancement degree <sup>b</sup>
1/36/female	Yes/yes	C6	Circular	No/no	Well defined	Low	Yes	Yes	Low SI with several isointense portions	Isointense with several high SI portions	Yes	Obvious
2/59/male	Yes/yes	C7	Circular	No/no	Well defined	Low	Yes	Yes	Low SI	Isointense with several high SI portions	Yes	—
3/77/female	Yes/yes	T5	Irregular	No/yes	Well defined	Low	Yes	Yes	Low SI	Isointense to high SI	Yes	Obvious
4/59/male	Yes/no	T11	Circular	Yes/no	Well defined	Low	Yes	Yes	—	—	—	—
5/39/female	No/yes	T12	Circular	No/no	—	—	—	—	Low SI with several isointense portions	Isointense with several high SI portions	Yes	—
6/22/male	No/yes	L3	Irregular	No/yes	—	—	—	—	Isointense to low SI	Low SI	No	—

<sup>a</sup>Compared with signal intensity and attenuation of the spinal cord, <sup>b</sup>Compared with signal intensity of the lesion on precontrast T1WI. CT: Computed tomography, MRI: Magnetic resonance imaging, GGO: Ground-glass opacity, SI: Signal intensity, —: nil



**Figure 2:** A 77-year-old female with monostotic fibrous dysplasia in T5 (original). (a) Axial computed tomography showed an irregular and expansile lesion. (b) Sagittal T1-weighted imaging magnetic resonance imaging showed low-signal intensity and partial vertebral collapse. (c) Sagittal T2-weighted imaging-FS magnetic resonance imaging showed isointense to high signal intensity. (d) Sagittal T1 weighted imaging-FS + C magnetic resonance imaging showed obvious and homogeneous enhancement.

## DISCUSSION

### Overview

FD occurrence in the spine is rare. Although MFD represents 70% of these lesions, involvement of axial bone is mostly seen in PFD. MFD involving the axial bone is extremely rare.<sup>[5,6,10,11]</sup> To the best of our knowledge, the characteristic radiographic appearances of MFD in long bones have been reported many times in the literature. However, only a few reports have described the imaging features of spinal MFD.<sup>[5,7,10,12,13]</sup>

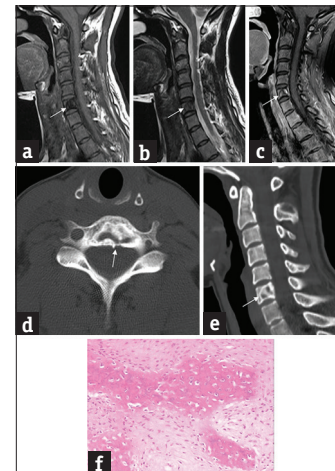


**Figure 3:** A 36-year-old female with monostotic fibrous dysplasia in C6 (original). (a) Sagittal T1-weighted imaging magnetic resonance imaging showed low-signal intensity with several isointense portions. (b) Sagittal T2-weighted imaging magnetic resonance imaging showed isointense with several high-signal intensity portions. (c) Sagittal T1-weighted imaging + C magnetic resonance imaging showed obvious and heterogeneous enhancement. (d) Axial computed tomography showed an expansile lesion and sclerotic rim. (e) Reformatted sagittal computed tomography showed the sclerotic rim more clearly. (f) Histopathology examination (H and E) showed delicate trabeculae of immature bone with no osteoblasts.

The present study reports the characteristic CT and MRI findings of six cases of MFD, with the aim of improving diagnostic accuracy.

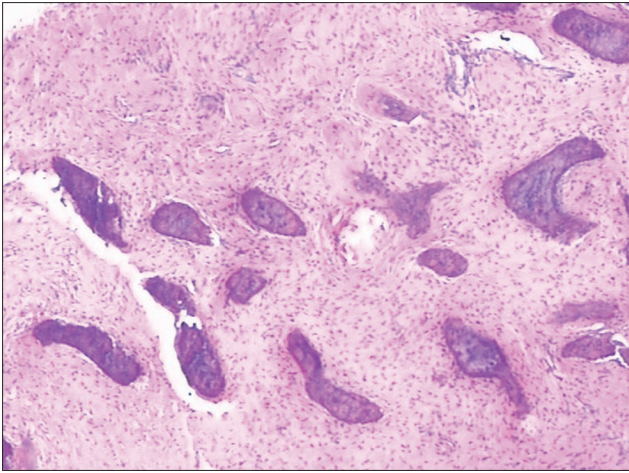


**Figure 4:** Histopathology examination (H and E) of a 59-year-old male with monostotic fibrous dysplasia in T11 (original). Histopathology examination showed delicate trabeculae of immature bone with no osteoblasts. The mesenchymal stroma surrounding the dysplastic trabeculae was relatively hypocellular and was composed of spindle-shaped primitive mesenchymal cells.

The peak incidence of the spinal MFD is the third-to-fifth decade of life, and no significant gender differences are seen.<sup>[5,14]</sup> In this study, patient age ranged from 22 to 77 years, with an average age of 48.7 years. The ratio of female-to-male patients (1:1) showed no relationship of disease to gender. These findings were in good agreement with values from the literature. The current literature shows that the spine, cervical, and lumbar vertebrae are the most commonly affected regions.<sup>[6]</sup> In this study, the lesions occurred in the cervical vertebra ( $n = 2$ ), thoracic vertebra ( $n = 3$ ), and lumbar vertebra ( $n = 1$ ). The incidence was different than other reports, which may be related to the number of cases. MFD also have the potential to be malignant (0.5%~3.4%). The most common type of malignant transformation is osteosarcoma.<sup>[7,15]</sup> Radiation therapy can significantly increase the probability of malignancy.<sup>[16]</sup> In this study, all patients were treated with surgical operation. Radiography was performed 3, 6, and 12 months after the surgery, every 6 months for the next 2 years, and annually thereafter. In the follow-up to this study, no recurrence or malignant tendency was found.

#### Etiologic and pathological changes

At present, the exact etiology of MFD is not clear. It is well-recognized that the etiology of MFD has been linked to an activating mutation of the Gs alpha gene on chromosome 20, which leads to an increase in cyclic adenosine monophosphate availability.<sup>[12]</sup>

MFD develops during skeletal development.<sup>[8]</sup> However, the clinical presentation depends on the location of the lesion.<sup>[8,12]</sup> Pain is usually proportional to the degree of vertebral body involvement.<sup>[7]</sup> Regarding pathology,

MFD is characterized by the replacement of bone marrow with poorly organized spicules of immature bone.<sup>[8,10]</sup> The combination of a lack of stress alignment and insufficient mineralization results in substantial loss of mechanical strength, leading to the development of pain, deformity, and vertebral collapse.<sup>[8]</sup> In this study, two cases had vertebral collapse. With the medical history of the patients, the backache both appeared 2 years ago without treatment.

#### Analysis of computed tomography imaging findings

The CT imaging features of spinal MFD depend on the underlying histopathology of the lesion.<sup>[3,5,17]</sup> Radiolucent areas are composed of fibrous elements, and radiopaque areas are composed of woven bone.<sup>[5]</sup> The normal bone is replaced by more radiolucent tissue and has a “ground-glass opacity (GGO)” pattern.<sup>[8]</sup> Another imaging feature of the lesion is the sclerotic rim. The lesion is bounded by a sclerotic rim of reactive bone. The sclerotic rim is defined more sharply on its inner border than its outer border.<sup>[8]</sup> In this study, the sclerotic rim and GGO were found in all cases. Spinal MFD has benign biological behavior, and the adjacent intervertebral disk can maintain its normal form. In this study, the adjacent bone was not involved in all cases.

Based on previous descriptions in the literature and the findings of the present study, spinal MFD has the following CT imaging findings: (1) expansile lesion, (2) well-defined margin and sclerotic rim, (3) GGO, (4) thinning of cortical bone, and (5) normal adjacent intervertebral disk.

#### Analysis of magnetic resonance imaging findings

MRI findings of spinal MFD in this study were nonspecific. Most lesions show low-signal intensity or low-signal intensity with several isointense portions on T1WI and isointense signal intensity with several high portions on T2WI. The cause of the heterogeneous signals may be related to the trabecular bone, cellularity, collagen fibers, cystic changes, and hemorrhage.<sup>[3,18]</sup> MFD may be surrounded by a layer of thick, sclerotic reactive bone, called a rind.<sup>[3]</sup> The rind can be seen as a dark signal rim on T1WI and T2WI.<sup>[3]</sup> Dark signal rims were found in four cases in this study. Two cases underwent enhanced MRI. The lesions showed obvious enhancement. Enhanced MRI can provide useful information regarding the quality of the blood supply and help to predict whether the lesion is benign.

#### Choice of imaging method

CT and MRI imaging have respective advantages in the diagnosis of spinal MFD. CT imaging can

**Table 2: The differential diagnosis of spinal monostotic fibrous dysplasia**

Characteristics	MFD	GCT	VH	ABC
Appearance	Expansile	Soap-bubble like	Corduroy-cloth like	Expansile
Ground-glass opacity	Yes	No	No	No
Sclerotic rim	Yes	No	Yes	Yes
Cortical destruction	No	Yes	No	Yes
Soft-tissue mass	No	Yes	No	Yes
MRI finding	Nonspecific	Low-to-isointense signal intensity on T1WI and T2WI	High-signal intensity on T1WI and T2WI	Fluid–fluid level

Yes: Common, No: Uncommon or not, MRI: Magnetic resonance imaging, MFD: Monostotic fibrous dysplasia, GCT: Giant cell tumor, VH: Vertebral hemangioma, ABC: Aneurysmal bone cyst

help evaluate the destruction of bone and provide accurate anatomical information to guide surgery.<sup>[3,5,7]</sup> MRI imaging can show the spinal cord and internal structures of the lesion more clearly. In summary, the combined use of CT and MRI examinations is necessary for patients with suspected spinal MFD. It should be mentioned that it will be quite difficult to diagnose spinal MFD with imaging studies when the vertebral body is collapsed.<sup>[3,11]</sup> In these cases, pathological examination should be taken into account.

### Differential diagnosis

The imaging findings of MFD are similar to other benign bony tumor-like lesions.<sup>[3,7,19,20]</sup> Differential diagnoses should include benign bony lesions such as (1) giant cell tumor (GCT); (2) vertebral hemangioma (VH); and (3) aneurysmal bone cyst (ABC). Table 2 described the differential diagnosis of spinal MFD.

GCT of the spine often shows expansile lesions and a “soap bubble” appearance.<sup>[21,22]</sup> In contrast to MFD, only a small number of lesions have a sclerotic rim. Cortical destruction was commonly seen in GCT.<sup>[21]</sup> On MRI, GCT often shows a heterogeneous or homogeneous signal intensity on T1WI. The solid areas of the tumor show heterogeneous low-to-intermediate signal intensity on T2WI.<sup>[23]</sup>

The “corduroy cloth” appearance is an important sign for VH, which represents the transverse cuts through the thickened vertical trabeculae.<sup>[24]</sup> On CT, the lesion is often nonexpanded and circular-like shape. On MRI, the lesion often shows high-signal intensity on T1WI and T2WI. Enhanced MRI imaging shows obvious enhancement.<sup>[25,26]</sup> Some scholars have suggested that the VH which causes nerve damage always shows a specific signal intensity (low signal intensity on T1WI and high signal intensity on T2WI).<sup>[25]</sup> This specific signal intensity is mainly due to the prominent hypervascular stroma.<sup>[26]</sup>

ABC of the spine often shows expansile lesion. The inner edge of the bone shell has different sizes of trace.<sup>[27]</sup> Lesions can breakthrough the cortical bone

to form soft-tissue masses. Due to the different components of the lesion, the lesion has various signal performances on MRI.<sup>[28]</sup> The presence of a “fluid–fluid” level on MRI is characteristic for ABC.<sup>[29]</sup> This feature is mainly due to the presence of blood in different stages of evolution.<sup>[29]</sup>

### Treatment

The treatment of spinal MFD still remains controversial. Some scholars have suggested that the treatment should focus on symptom relief and prevention of lesion progression rather than a simple resection.<sup>[5]</sup> It is well-recognized that bisphosphonates as a first-line drug have successfully relieved the pain.<sup>[5,10,12]</sup> However, once medical management fails, surgical management should be taken into consideration. The purpose of surgery is to reconstruct the stability of the vertebral body, and the most frequently used methods are curettage, internal fixation, and bone grafting.<sup>[11]</sup>

### CONCLUSIONS

The CT and MRI manifestations of spinal MFD have the following characteristics: expansile lesions, GGO, sclerotic rims, and no obvious soft-tissue masses. These features can provide a highly suggestive diagnosis of spinal MFD. In addition, the combined use of CT and MRI examinations is necessary for patients with suspected spinal MFD.

### Financial support and sponsorship

Nil.

### Conflicts of interest

There are no conflicts of interest.

### REFERENCES

- Lichtenstein L. Polyostotic fibrous dysplasia. *Arch Surg* 1938;36:874-98.
- Lichtenstein L, Jaffe H. Fibrous dysplasia of bone. *Arch Pathol* 1942;33:777-816.
- Park SK, Lee IS, Choi JY, Cho KH, Suh KJ, Lee JW, et al. CT and MRI of fibrous dysplasia of the spine. *Br J Radiol* 2012;85:996-1001.
- Samdani A, Torre-Healy A, Chou D, Cahill AM, Storm PB.

- Treatment of osteblastoma at C7: A multidisciplinary approach. A case report and review of the literature. *Eur Spine J* 2009;18 Suppl 2:196-200.
5. Wu FL, Jiang L, Liu C, Yang SM, Wei F, Dang L, et al. Fibrous dysplasia of the mobile spine: Report of 8 cases and review of the literature. *Spine (Phila Pa 1976)* 2013;38:2016-22.
  6. Harris WH, Dudley HR Jr., Barry RJ. The natural history of fibrous dysplasia. An orthopaedic, pathological, and roentgenographic study. *J Bone Joint Surg Am* 1962;44-A: 207-33.
  7. Sharifudin MA, Zakaria Z, Awang MS, Mohamed Amin MA, Abd Aziz A. A rare case of monostotic spinal fibrous dysplasia mimicking solitary metastatic lesion of thyroid carcinoma. *Malays J Med Sci* 2016;23:82-6.
  8. DiCaprio MR, Enneking WF. Fibrous dysplasia. Pathophysiology, evaluation, and treatment. *J Bone Joint Surg Am* 2005;87:1848-64.
  9. Ippolito E, Bray EW, Corsi A, De Maio F, Exner UG, Robey PG, et al. Natural history and treatment of fibrous dysplasia of bone: A multicenter clinicopathologic study promoted by the european pediatric orthopaedic society. *J Pediatr Orthop B* 2003;12:155-77.
  10. Ren K, Lan T, Yu Z, Chen Y, Tian CQ, Gu HS, et al. Monostotic fibrous dysplasia of the thoracic spine: A case report. *J Back Musculoskelet Rehabil* 2016;29:387-91.
  11. Tezer M, Erturer E, Ozturk C, Aydogan M, Hamzaoglu A. Symptomatic polyostotic fibrous dysplasia of the thoracic spine. *Joint Bone Spine* 2006;73:742-4.
  12. Schoenfeld AJ, Koplun SA, Garcia R, Hornicek FJ, Mankin HJ, Raskin KA, et al. Monostotic fibrous dysplasia of the spine: A report of seven cases. *J Bone Joint Surg Am* 2010;92:984-8.
  13. Yang C, Zhu B, Chen A. Imaging diagnosis of monostotic fibrous dysplasia in thoracic and lumbar spine vertebrae. *J Huazhong Univ Sci Technolog Med Sci* 2007;27:684-6.
  14. Meredith DS, Healey JH. Twenty-year follow-up of monostotic fibrous dysplasia of the second cervical vertebra: A case report and review of the literature. *J Bone Joint Surg Am* 2011;93:e74.
  15. Fu CJ, Hsu CY, Shih TT, Wu MZ. Monostotic fibrous dysplasia of the thoracic spine with malignant transformation. *J Formos Med Assoc* 2004;103:711-4.
  16. Kim GT, Lee JK, Choi BJ, Kim J, Han SH, Kwon YD, et al. Malignant transformation of monostotic fibrous dysplasia in the mandible. *J Craniofac Surg* 2010;21:601-3.
  17. Fitzpatrick KA, Taljanovic MS, Speer DP, Graham AR, Jacobson JA, Barnes GR, et al. Imaging findings of fibrous dysplasia with histopathologic and intraoperative correlation. *AJR Am J Roentgenol* 2004;182:1389-98.
  18. Parekh SG, Donthineni-Rao R, Ricchetti E, Lackman RD. Fibrous dysplasia. *J Am Acad Orthop Surg* 2004;12:305-13.
  19. Wright JF, Stoker DJ. Fibrous dysplasia of the spine. *Clin Radiol* 1988;39:523-7.
  20. Ehara S, Kattapuram SV, Rosenberg AE. Fibrous dysplasia of the spine. *Spine (Phila Pa 1976)* 1992;17:977-9.
  21. Si MJ, Wang CG, Wang CS, Du LJ, Ding XY, Zhang WB, et al. Giant cell tumours of the mobile spine: Characteristic imaging features and differential diagnosis. *Radiol Med* 2014;119:681-93.
  22. Sigwalt L, Bourgeois E, Eid A, Durand C, Griffet J, Courvoisier A, et al. A thoracic spinal bone giant cell tumor in a skeletally immature girl. A case report and literature review. *Childs Nerv Syst* 2016;32:873-6.
  23. Alfawareh MD, Shah ID, Orief TI, Halawani MM, Attia WI, Almusrea KN, et al. Pediatric upper cervical spine giant cell tumor: Case report. *Global Spine J* 2015;5:e28-33.
  24. Gaudino S, Martucci M, Colantonio R, Lozupone E, Visconti E, Leone A, et al. A systematic approach to vertebral hemangioma. *Skeletal Radiol* 2015;44:25-36.
  25. Castel E, Lazennec JY, Chiras J, Enkaoua E, Saillant G. Acute spinal cord compression due to intraspinal bleeding from a vertebral hemangioma: Two case-reports. *Eur Spine J* 1999;8:244-8.
  26. Alfawareh M, Alotaibi T, Labeed A, Audat Z. A symptomatic case of thoracic vertebral hemangioma causing lower limb spastic paresis. *Am J Case Rep* 2016;17:805-9.
  27. Sebaaly A, Ghostine B, Kreichati G, Mallet JF, Glorion C, Moussa R, et al. Aneurysmal bone cyst of the cervical spine in children: A review and a focus on available treatment options. *J Pediatr Orthop* 2015;35:693-702.
  28. Chan MS, Wong YC, Yuen MK, Lam D. Spinal aneurysmal bone cyst causing acute cord compression without vertebral collapse: CT and MRI findings. *Pediatr Radiol* 2002;32:601-4.
  29. Cugati G, Pande A, Jain PK, Symss NP, Ramamurthi R, Vasudevan CM, et al. Aneurysmal bone cyst of the lumbar spine. *Asian J Neurosurg* 2015;10:216-8.